Seminars in Arthroplasty 34 (2024) 698–707

Available online at www.sciencedirect.com

ScienceDirect

www.jsesarthroplasty.org

Prediction of premorbid three-dimensional anatomy of the glenoid based on statistical shape modeling

Jean-David Werthel, MD, PhD[a,*], Théo Giraudon, MSc[b], Gilles Walch, MD[c], Cole T. Fleet, MESc[d], Manuel Urvoy, PhD[b], Yannick Morvan, PhD[b], and Arnaud Walch, MD[e]

[a]Orthopedic Department, Hôpital Ambroise Paré, Boulogne-Billancourt, France
[b]Imascap, Plouzané, France
[c]Ramsay Générale de Santé, Jean Mermoz Private Hospital, Centre Orthopédique Santy, Lyon, France
[d]Roth McFarlane Hand and Upper Limb Centre, Biomechanics Laboratory - University of Western Ontario, London, ON, Canada
[e]Orthopedic Department, Hôpital Edouard Herriot, Lyon, France

A R T I C L E I N F O

Keywords:
3D preoperative planning
3D reconstruction
Prediction
Glenoid geometry
Statistical shape modeling
Lateral offset
Lateralization

A B S T R A C T

Background: Restoration of an anatomic joint line after anatomic total shoulder arthroplasty and of the optimal lateral offset after reverse total shoulder arthroplasty may be relatively straightforward when the glenoid does not present with severe erosion. However, in cases of severe glenoid bone loss, the surgeon is left with no preoperative landmark to restore these parameters. The objective of this study was to use statistical shape modeling, to predict the premorbid morphology of the glenoid. We hypothesized that this would allow us to accurately determine premorbid glenoid version and inclination, in addition to accurately quantifying bone loss and medialization.

Methods: Fifty-six bilateral computed tomography scans of the shoulders of patients scheduled for shoulder arthroplasty and determined to have unilateral osteoarthritis (primary osteoarthritis or cuff tear arthropathy with a healthy contralateral side) were obtained. A statistical shape model was automatically applied on the pathologic arthritic side to predict its premorbid anatomy. Glenoid version, inclination, height, width, and glenoid and scapula lateral offset were measured automatically. These measurements were obtained on the pathological arthritic cases, on the contralateral control healthy cases, and on the premorbid predictions of the pathological arthritic cases and were compared pair by pair.

Results: The mean difference between the pathological arthritic side and the contralateral healthy side was 9.1° ± 7.3° for version, 4.8° ± 4.8° for inclination, 4.9 ± 4.5 mm for height,

This study was approved by the Institutional Review Board of the Ethical Committee of Hôpital Privé Jean Mermoz, Lyon, France (COS-RGDS-2020-05-001-WALCH-G). All patients provided informed consent. Each author certifies that his or her institution approved the human protocol for this investigation and that all investigations were conducted in conformity with ethical principles of research.

*Corresponding author: Jean-David Werthel, MD, PhD, Hôpital Ambroise Paré, 9 Avenue Charles de Gaulle, Boulogne-Billancourt, 92100, France.

E-mail address: jdwerthel@gmail.com (J.-D. Werthel).

https://doi.org/10.1053/j.sart.2024.04.001

4.7 ± 5.3 mm for width, 2.4 ± 1.9 mm for scapula lateral offset, and the glenoid lateral offset was 1.5 ± 1.5 mm. The mean difference between the premorbid prediction of the pathological side and the contralateral healthy side was reduced to 3.3° ± 2.4° for version, 3.4° ± 2.6° for inclination, 3.0 ± 1.9 mm for height, 2.3 ± 1.4 mm for width, 2.2 ± 1.7 mm for scapula lateral offset, and the glenoid lateral offset was 0.9 ± 0.8 mm.

Conclusion: This study shows that statistical shape modeling can allow accurate prediction of the premorbid morphology of the glenoid. This could help optimize implant selection and positioning after anatomic total shoulder arthroplasty and reverse total shoulder arthroplasty to restore optimal soft-tissue tension.

Level of evidence: Basic Science Study; Computer Modeling

In the past decade, Iannotti et al[27,31,40] demonstrated that 3-dimensional (3D) preoperative planning allowed better accuracy and reproducibility in the positioning of shoulder arthroplasty implants than 2-dimensional (2D) computed tomography (CT) scan planning. Since then, numerous different planning systems have been created. These allow 3D reconstruction of the scapula and of the humerus, precise calculation of glenoid version, inclination and humeral subluxation, and virtual implantation of a shoulder arthroplasty and even simulation of impingement-free passive motion with the implants in place.[11]

Optimal positioning of the implants and especially of the glenoid implant has been shown to be crucial in obtaining optimal function and survivorship after both anatomic total shoulder arthroplasty (aTSA)[13,46] and reverse total shoulder arthroplasty (rTSA).[9,21,35]

In the setting of aTSA, it has been proven that functional results after aTSA are correlated to the accurate reproduction of the center of rotation of the shoulder to reproduce normal glenohumeral kinematics and ideal tensioning of the rotator cuff.[42,49] Excessive lateralization of the joint may lead to overtensioning of the joint, of the rotator cuff, and of the subscapularis repair. This may in turn lead to reduced range of motion and strength, and increased glenohumeral joint reaction forces with subsequent polyethylene wear and aseptic glenoid loosening.[30,43,48] On the opposite, excessive medialization of the joint line may also have detrimental effects as it may medialize and shorten the rotator cuff. This could result in worse functional outcomes and could be a contributing factor for recurrent posterior subluxation.[6,28] Ho et al recently demonstrated that increased preoperative medialization of the joint line was associated with increased central peg osteolysis despite appropriate restoration of version and inclination.[25] Therefore, it appears that in the setting of aTSA, correction of version and inclination may not be enough to obtain optimal function and longevity of the implants and it is probably as important to also restore and normalize the joint line.

In the setting of rTSA, restoration of an appropriate lateral offset also appears necessary to restore optimal soft-tissue tension. Numerous recent studies have analyzed the effects of lateralization after rTSA which can be influenced by implant design, implant positioning, and humeral cut but also by preoperative glenoid erosion.[47] Therefore, precise preoperative assessment of the amount of glenoid erosion appears to be necessary to restore optimal soft-tissue tension after implantation of the rTSA.

Restoration of an anatomic joint line after aTSA and of the optimal lateral offset after rTSA may be relatively straightforward when the glenoid does not present with severe erosion. However, in cases of severe glenoid bone loss, the surgeon is left with no preoperative landmark to restore these parameters. The objective of this study was to use statistical shape modeling (SSM), to predict the premorbid morphology of the glenoid. We hypothesized that this would allow us to accurately determine premorbid glenoid version and inclination, in addition to accurately quantifying bone loss and medialization.

Materials and methods

This study was approved by the Institutional Review Board of the Ethical Committee of Hôpital Privé Jean Mermoz, Lyon, France (COS-RGDS-2020-05-001-WALCH-G). All patients provided informed consent.

Study cohort

Bilateral CT scans of the shoulders of patients scheduled for shoulder arthroplasty and determined to have unilateral osteoarthritis (OA) (primary OA, cuff tear arthropathy, posttraumatic arthropathy) were acquired in 1 of 9 different institutions between September 2015 and June 2023 with the following acquisition parameters: slice thickness <1.2 mm, number of slices >200, field of view: whole scapula, X-Y resolution <0.5 mm, matrix size: 512 × 512 and kV140, and mA > 300. All CT scans were uploaded in a validated automated software for 3D preoperative planning (BluePrint, v2.1.6; Tornier, France). All cases were reviewed by 2 shoulder surgeons (G.W. and J.D.W.). The pathologic arthritic sides were classified using the reformatted 2D and 3D reconstructions obtained with the software according to the Walch classification for OA[2,45] and to the Favard classification for cuff tear arthropathy.[41] The contralateral healthy sides were all verified to exclude any cases with evidence of glenoid erosion,

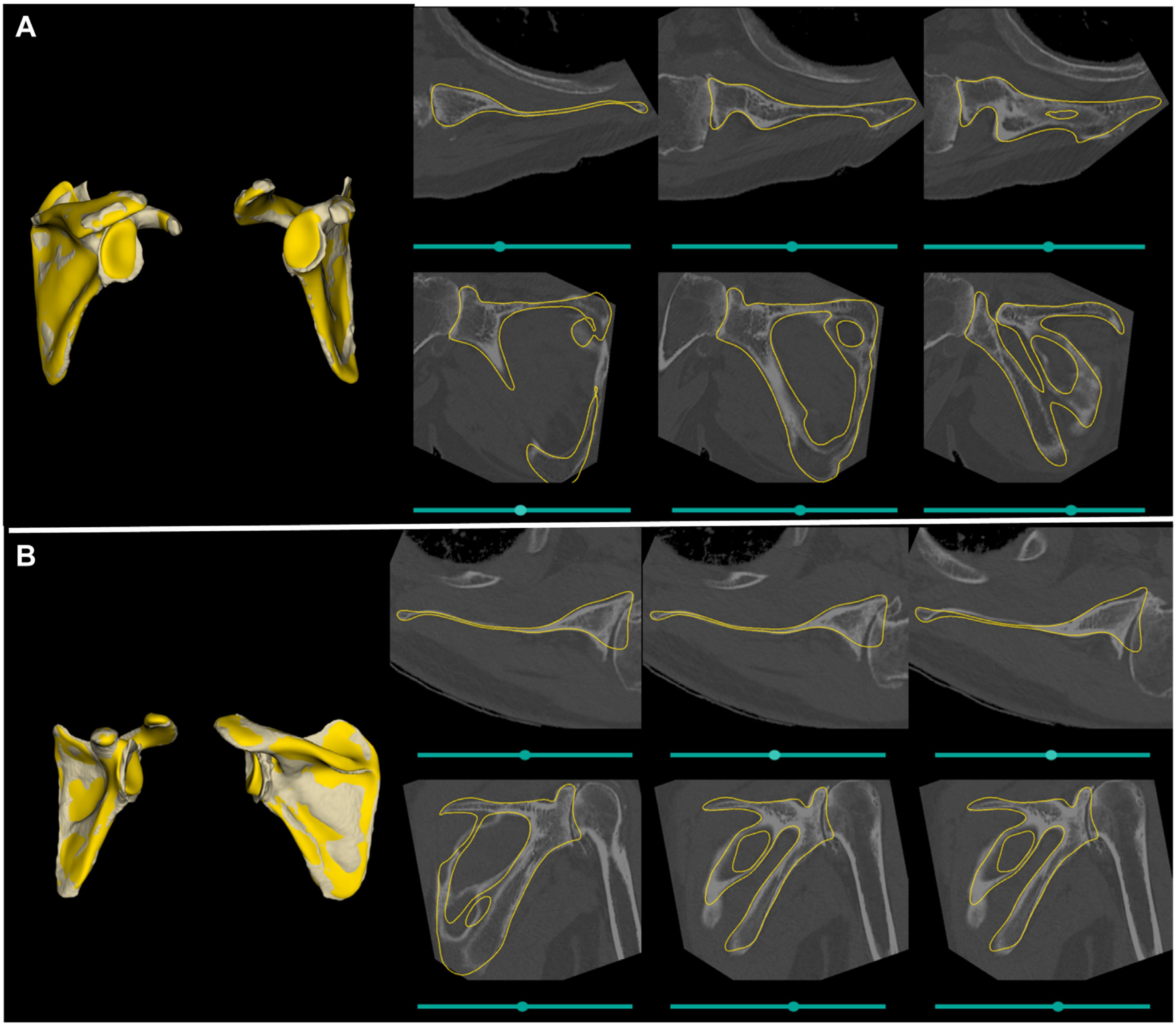

Figure 1 – Examples of reconstruction of the premorbid anatomy of the scapula using a statistical shape model. 2D and 3D reconstructions of an arthritic scapula and of the premorbid model in yellow. (A) Right shoulder with an A1 glenoid according to the Walch classification. (B) Left shoulder with a B3 glenoid according to the Walch classification.

glenohumeral OA, rotator cuff muscles fatty infiltration, or any other disorder of the shoulder. Any discordance was resolved by consensus of the surgeons. Patients were excluded if the contralateral shoulder (scapula or humerus) presented any sign of abnormality, dysplasia, prior trauma, or arthritis and if the scapula was truncated.

Prediction of the premorbid morphology of the glenoid

SSM is a shape analysis algorithm that aims at capturing the most significant shape variations in a collection of 2D or 3D shapes.[8] This technique is here applied to a cohort of healthy scapula bones. The analysis is performed by accumulating these scapulae shapes to generate 1 3D mean shape associated with shape variation descriptors. These descriptors are based on so-called eigenvectors, enabling them to capture the shape variations of the initial collection. The eigenvalues associated with the eigenvectors represent the amplitude of these variations. The capability of reconstructing a shape constitutes the major advantage employed in this study as it enables the reconstruction of a healthy 3D scapula shape while completing or predicting any missing part (Fig. 1). In the context of this study, the reconstruction primarily relies on the medial scapula which is less susceptible to arthritic changes while predicting the native shape of the glenoid prior to any injury or disease.

To create our scapula SSM, a database of 85 3D shapes of healthy scapulae was created. None of these healthy scapulae were used in the present study to avoid any bias related to the validation of the prediction accuracy. These 3D shapes were obtained by manual segmentation of the scapulae using the Amira 5.3.3 software (VSG - Visualization Sciences Group, Burlington, MA, USA). This allowed the creation of 3D shape models from the segmentation mask. There were 59 right scapulae and 26 left scapulae. The scapula collection was exclusively formed of right scapulae by mirroring the left scapulae along the sagittal plane.

The training dataset/sample pool employed to build the SSM is based on a database of 85 nonarthritic, healthy patients. This sample size falls within the recommended range of 60 to 100 samples for creating SSMs of bone structures because this covers the most important structure variations in a given cohort. In addition, such a sufficient coverage is confirmed by the final results on the testing dataset. Specifically, the testing dataset/sample pool consisted of n = 56 strictly normal contralateral CT scans (36 females and 20 males, with a mean age of 72.39 years and a standard deviation of 9.05). To study the statistical power, we assumed that the distributions of measurements for the premorbid and contralateral sides would be similar to those reported by Giraudon et al.[17] Based on the Minimal Detectable Change (MDC) defined in this study, we determined the minimum clinically acceptable difference we wanted to detect (5° for version and inclination, 2 mm for height and width, and 3 mm for the scapula offset). As a result, the desired testing sample size was as follows:

- 9 pairs for the inclination
- 10 pairs for the version
- 20 pairs for the height
- 15 pairs for the width
- 45 pairs for the scapula offset

As a result, the greatest desired sample size was n = 45. This size is smaller than the total number of contralateral CT scans, which makes the testing dataset capable of detecting MDCs.

Measurements

Glenoid version, inclination, width, height, and lateral offset were automatically computed using the Blueprint 3D-planning software.[4] The lateral offset of a given subject was measured using 2 different methods: the scapula lateral offset and the glenoid lateral offset.

The scapula lateral offset is intrinsic to a given scapula. It was defined as the distance between the glenoid center and the most medial point of the trigonum scapulae projected on the transverse axis (Fig. 2).

The glenoid lateral offset compares the lateral offset of 2 scapulae (eg, arthritic vs. healthy and healthy vs. premorbid). The 2 compared scapulae were automatically aligned without considering the glenoid articular surface. Then the distance between the projection of the vector of the 2 glenoid centers onto the transverse axis of 1 scapula was measured. To compare the healthy scapula with the contralateral side (arthritic or the premorbid scapula), the healthy scapula was mirrored to align it with the contralateral side (Fig. 3).

These measurements were obtained on the pathological arthritic cases, on the contralateral control healthy cases, and on the premorbid predictions of the pathological arthritic cases. The premorbid predictions of the pathological side were compared with the contralateral healthy shoulder for all cases to validate the premorbid prediction tool as Verhaegen et al[44] have demonstrated that the contralateral healthy side can be used as a template to determine premorbid anatomy.

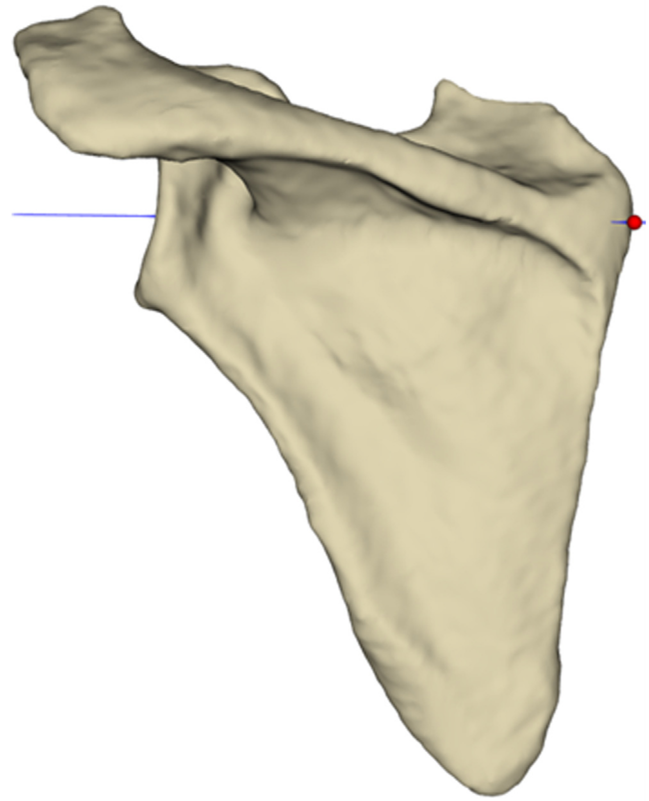

Figure 2 – Scapula lateral offset: defined as the distance between the glenoid center and the most medial point of the trigonum scapulae (●) projected onto the transverse axis (–).

Statistical analysis

Before comparing the arthritic and healthy measurements and the premorbid and healthy measurements, Shapiro-Wilk tests were performed to evaluate the normality of these paired differences. The *t*-test was chosen for paired differences following a normal distribution, and a Wilcoxon test for the other ones.

Descriptive statistics were calculated, including means, standard deviation, and minimum and maximum values of continuous variables. Normal distribution of data was tested according to the Shapiro-Wilk test and the Levene's test. Dependent samples were compared by use of a paired *t*-test and by the Wilcoxon signed-rank test according to data distribution. The level of statistical significance was set at $P < .05$. Statistical analyses were performed with the R package version 4.2.1 (R Foundation for Statistical Computing, Vienna, Austria).

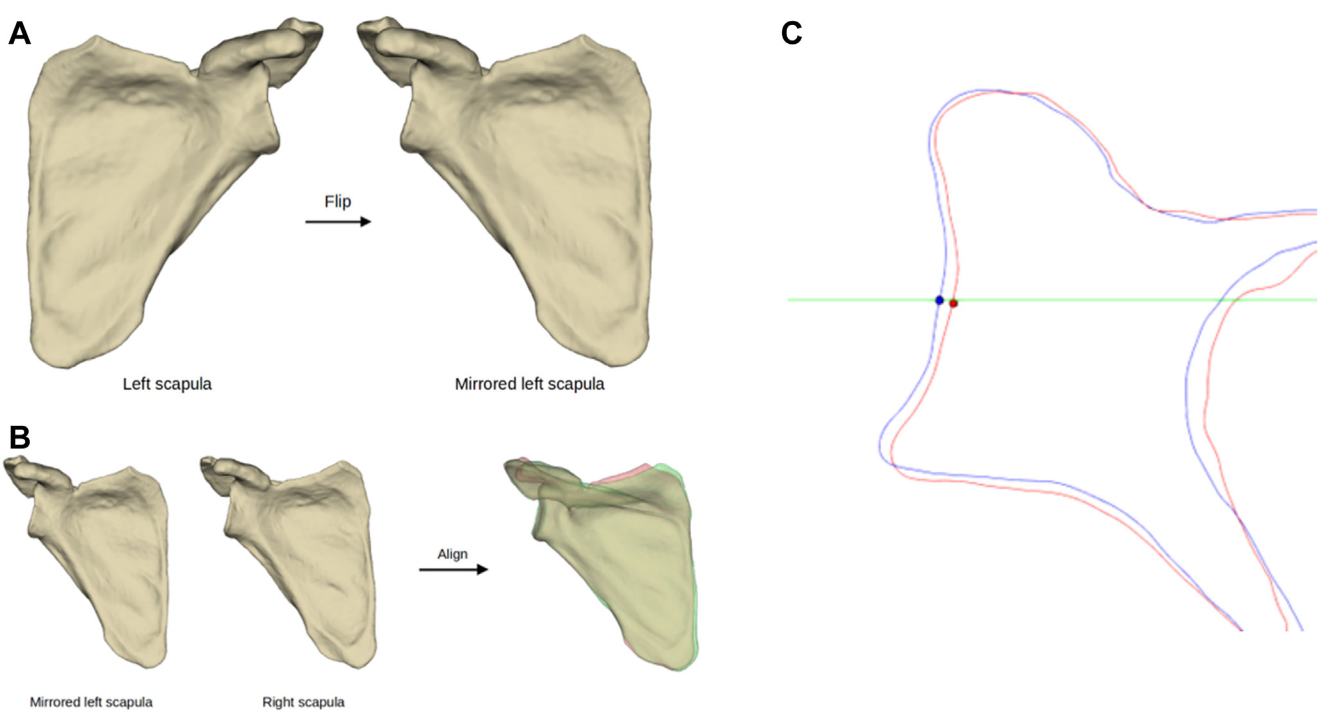

Figure 3 – Glenoid lateral offset: The healthy left scapula is mirrored (A) and aligned automatically to the pathologic contralateral scapula without considering the glenoid articular surface (B). The distance between the projection of the vector of the 2 glenoid centers on the transverse axis of one scapula corresponds to the glenoid lateral offset (C).

Results

Study cohort

A total of 294 patients with bilateral CT scans were included. Among these, 238 patients were excluded due to evidence of pathology on the contralateral control side or truncated CT scans, leaving 56 patients for analysis (19% of the cases).

There were 41 cases of OA (2 A1, 6 A2, 1 B1, 19 B2, 10 B3, 3 D), 14 cases of cuff tear arthropathy (4 E1, 6 E2, 4 E3), and 1 locked posterior shoulder dislocation. Mean glenoid version, inclination, height and width, and scapula lateral offset in the 3 groups are reported in Table I.

Measurements

The mean differences for all outcome variables for the pathologic and premorbid prediction groups when compared to the contralateral healthy group are reported in Table II. The mean glenoid lateral offset is additionally reported for each group.

Table I – Glenoid parameters (mean ± 1 SD) in arthritic shoulders, healthy contralateral controls, and premorbid predictions of the arthritic shoulders.

	Arthritic	Healthy	Premorbid prediction
Version (°)	−13.2 ± 12.3	−7.8 ± 4.7	−7.1 ± 3.7
Inclination (°)	3.0 ± 6.7	6.9 ± 5.5	6.3 ± 4.2
Height (mm)	39.5 ± 5.4	34.7 ± 3.2	37.4 ± 3.3
Width (mm)	30.6 ± 6.3	26.3 ± 3.3	28.1 ± 2.7
Scapula lateral offset (mm)	102.1 ± 7.8	103.9 ± 7.4	103.1 ± 7.4

SD, standard deviation.

Discussion

This study showed SSM to be an accurate method for predicting the premorbid anatomy of the glenoid in patients' severe glenoid bone loss. This could help surgeons improve their preoperative plan to better understand and restore patients' anatomy in a more precise manner and serve as a guide for optimal implant selection and positioning. Indeed, it has been proven that the objective after aTSA is to restore neutral glenoid version.[36] However, the objective of glenoid inclination remains unclear and accurate prediction of patients' premorbid inclination could help determine such objectives. In addition, glenoid erosion is often observed in arthritic shoulders leading to medialization of the joint line. Such medialization may lead to excessive laxity in the soft tissue and potentially early glenoid loosening due to eccentric loading of the glenoid implant. Several different techniques exist to correct glenoid retroversion. These typically include eccentric anterior reaming,[33] posterior glenoid bone grafting,[24] or augmented glenoid implants[29] which have shown mixed results and allow different amounts of restoration of the anatomic joint line. Precise prediction of patients' premorbid anatomy can therefore help in selecting the most adapted technique to restore optimal kinematics and survivorship to the shoulder after aTSA.

Table II – Mean differences (mean ± 1 SD) in glenoid parameters between arthritic shoulders, healthy contralateral controls, and premorbid predictions of the arthritic shoulders.

	Healthy vs. arthritic		Healthy vs. premorbid prediction	
	Difference	*P* value	Difference	*P* value
Version (°)	9.1 ± 7.3	<.01 (w)	3.3 ± 2.4	.21 (t)
Inclination (°)	4.8 ± 4.8	<.01 (w)	3.4 ± 2.6	.20 (t)
Height (mm)	4.9 ± 4.5	<.01 (w)	3.0 ± 1.9	<.01 (t)
Width (mm)	4.7 ± 5.3	<.01 (w)	2.3 ± 1.4	<.01 (w)
Scapula lateral offset (mm)	2.4 ± 1.9	<.01 (t)	2.2 ± 1.7	.05 (t)
Glenoid offset lateral (mm)	1.5 ± 1.5	N/A	0.9 ± 0.8	N/A

N/A, not applicable; *SD*, standard deviation.
(t) indicates a *P* value computed with a *t*-test and (w) indicates a *P* value computed with a Wilcoxon test.

Similarly after rTSA, it has been proven that the glenoid baseplate should be positioned flush to the inferior glenoid rim,[20] with a reverse shoulder arthroplasty angle of 0°.[5] However, the optimal version of the glenoid baseplate remains unknown, although neutral version is often recommended. Recently, Keener et al[32] showed little to no effect of glenoid baseplate version on passive glenohumeral impingement-free range of motion on a computer model. In addition, Friedman et al[14] found in a finite element analysis that a glenoid baseplate could tolerate up to 25° of retroversion to allow for bony ingrowth to occur. These findings were confirmed in a clinical study where no significant difference in postoperative functional outcomes, range of motion, or complications between patients who had baseplate retroversion ≤15° vs. those who had retroversion >15° could be found at a 2-year follow-up.[10]

Nevertheless, the biggest unknown parameter when planning for rTSA is what to aim for in terms of lateralization. While it is clear that some amount of glenoid lateralization is necessary to improve impingement-free range of motion and to decrease the risk of scapular notching,[47] the optimal final position of the humerus relative to the scapula after rTSA remains unknown. Indeed, excessive medialization might lead to soft-tissue laxity, instability, and decrease in deltoid moment arm, whereas excessive lateralization could lead to excessive tension, difficulty to reduce the joint, polyethylene wear, pain, acromial stress fracture, and nerve injury. In addition, it remains unknown whether the same amount of lateralization should be applied when implanting an rTSA on a shoulder with or without a well-functioning rotator cuff and whether this parameter should vary depending on the amount of remaining cuff and/or depending on the deltoid volume and shape. Numerous biomechanical[15,16,19,23,26] and clinical studies have attempted to analyze the effects of humeral, glenoid, and global lateralization after rTSA. Most of these studies have shown that a lateralized design possibly leads to decreased scapular notching with slightly better range of motion especially in external and internal rotation.[12,18,22,34] However, these studies focus on comparing the outcomes after different designs of implants but do not consider the preoperative lateral offset of each patient which depends on the diameter of humeral head and on the amount of glenoid erosion. Without this information, it is not possible to know how the postoperative lateral offset after rTSA of a given patient compares to his native anatomical premorbid lateral offset (Fig. 4). To this date, the ideal lateral offset after rTSA is still not known,[3] although we can suppose that the ideal postoperative soft-tissue tension could be obtained by restoring the anatomical premorbid position of the tuberosities.

Several other methods have been published to predict the premorbid anatomy of the glenoid. Verhaegen et al[44] have demonstrated that the contralateral healthy side could be used as a surrogate for the premorbid anatomy of the pathological side as they found a mean difference of 2 mm in offset, 2° in inclination, and 2° in version between scapula pairs in healthy nonarthritic individuals. However, it is difficult to obtain bilateral CT scans in routine practice. Furthermore, in most cases of glenohumeral arthritis, the contralateral side has also undergone arthritic changes making this method difficult to generalize. In addition, Giraudon et al[17] in a larger study of 130 pairs of healthy scapulae found similar results with very strong intraclass correlation coefficients between left and right shoulders for all evaluated paired measures and low differences between the means of glenoid version, inclination, height, width, and scapula lateral offset which were found to be always inferior to the MDC. Nevertheless, although the differences between left and right shoulders were very small at the scale of the scapula, these were all statistically significant except for glenoid height. Therefore, our statistical shape model appears to be as accurate in predicting scapular premorbid anatomy as using the contralateral scapula. In 2008, Codsi et al[7] and Scalise et al[39,40] demonstrated that the endosteal surface of the glenoid defined as the "glenoid vault" is a highly consistent shape in healthy individuals. They showed that this glenoid vault can be reliably used to predict premorbid anatomy of the glenoid by manually aligning and rescaling this vault model in a best-fit manner with the remaining portions of the eroded glenoid bone. As opposed to the proposed SSM-based method, the vault model proposed by Codsi et al[7] and Scalise et al[39,40] relies on a nondeformable and fixed size 3D template model of the scapula vault. While presenting the advantage of simplicity, the vault model cannot capture and describe the variations of scapular shapes. Conversely, an SSM is based on the combination of (1) a fixed-size mean 3D template and (2) metadata (eigenvectors and eigenvalues) describing the shape variations. As a result, a deformable SSM offers greater shape description capabilities compared to a fixed-size 3D template. Abler et al[1] proposed a method to predict premorbid glenoid anatomy based on a local statistical shape model including the glenoid, parts of the acromion, and coracoid. They found that this technique could predict the overall surface of a healthy scapula with an accuracy of 2.3° ± 1.8° for glenoid version, 2.1° ± 2.0° for inclination, and 0.7 ± 0.5 mm for medialization of the joint line. In their study, they used a leave-one-out method to report the reconstruction error of their model. However, this method does not validate the

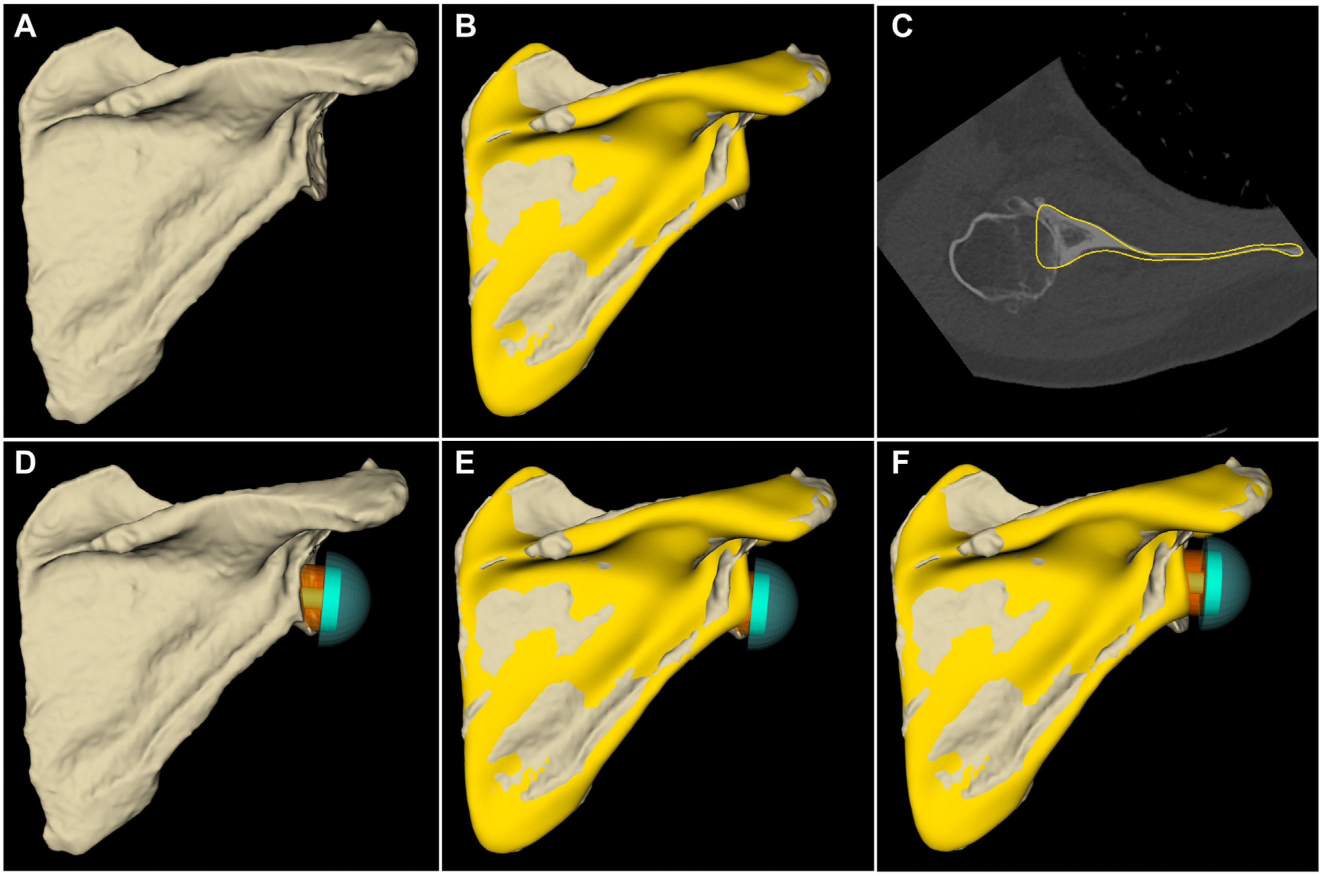

Figure 4 – Example of a right shoulder with a B3 glenoid (24° of retroversion, 82% of posterior humeral subluxation). (A) Posterior view of the 3D reconstruction of the scapula. (B) Posterior view of the 3D reconstruction of the premorbid anatomy of the scapula. (C) Axial 2D CT view of the scapula and of the premorbid prediction of the scapula in yellow. (D) Preoperative plan of a glenoid baseplate with an angled BIO-RSA graft (12.5°, 6 mm thick on the thin side and 12.5 mm on the thick side). The baseplate is positioned flush to the inferior rim of the glenoid. The graft compensates for the posterior erosion. (E) Preoperative plan of a glenoid baseplate with a similar angled BIO-RSA graft but this time on the premorbid reconstruction of the scapula. The graft does not provide any glenoid lateralization. In addition, the premorbid prediction helps the surgeon identify an inferior osteophyte. (F) Modified preoperative plan of a glenoid baseplate with a similar angled BIO-RSA based on the information provided by the premorbid prediction of the scapula to achieve some amount of glenoid lateralization in addition to the compensation of the posterior bone loss.

accuracy of the shape model in its ability to determine premorbid anatomy for individual OA glenoids. Similarly, Plessers et al[37] and Salhi et al[38] reported similar accuracy to reconstruct artificial defects manually created using a statistical shape model of the entire scapula.

All these methods are comparable to our fully automatized method. In addition, in most of the studies aforementioned, no statistical analysis was performed. Therefore, although minimal differences were found, these were never described as being statistically significant. Our study shows that the use of a statistical shape model would predict premorbid anatomy with an average precision which is well below the precision offered by preoperative planning software coupled with patients-specific instrumentation. This method can easily be used in routine practice as a guide for implant positioning and selection in both aTSA and rTSA. However, while this premorbid prediction might be sufficient for aTSA, additional studies are warranted to better understand the amount of lateralization needed after rTSA. Reconstruction of the premorbid anatomy of the eroded glenoid will allow us to determine a reference point when measuring the lateral offset after rTSA.

This study has several limitations. First, the sample size of 56 bilateral cases is relatively small. This was due to the difficulty in obtaining bilateral CT scans with unilateral OA. Second, we assumed that the contralateral healthy side could be used as a template for the premorbid anatomy of the pathological side based on the work of Verhaegen et al.[44] However, there might be some differences between left and right scapulae based on arm dominance. Third, a statistical shape model has some specificities which need to be understood. Indeed, it may be better at predicting version, inclination, and scapular lateral offset than glenoid lateral offset, height, and width as shown in Table II. However, one strength of the statistical shape model lies in its ability to capture smooth shape variations, enabling a precise prediction of the shape and location of the glenoid surface center. This strength is key to precisely predict the scapular offset. Conversely, the statistical shape model has more difficulties in capturing sharp shape variations effectively. When comparing the healthy and premorbid prediction of version and inclination, this results in a P value of .21 and .20, respectively. However, these quantitative differences are as low as $3.3^\circ \pm 2.4^\circ$ and $3.4^\circ \pm 2.6^\circ$, for version and inclination, respectively. This indicates that the statistical distribution of the predicted version and inclination is similar to that of healthy scapulae. This is confirmed in Table I, which provides the statistics of the predicted version and inclination. In addition, the quantitative differences between the healthy and premorbid prediction of version and inclination ($3.3^\circ \pm 2.4^\circ$ and $3.4^\circ \pm 2.6^\circ$) are deemed acceptable considering the targeted clinical precision. Finally, we chose to include 2 different methods of measurement of the lateral offset. Both methods have advantages and disadvantages. The measure of the scapula lateral offset allows for easy comparison between 2 existing scapulae, as it avoids the alignment process (described in Fig. 3) which could be a potential source of bias. However, the glenoid offset allows easy comparison between a pathological glenoid and its premorbid reconstruction and has the advantage of working on truncated scapulae. However, it relies on an alignment process, while the scapula offset is simpler and intrinsic to a given scapula.

Conclusion

This study shows that SSM can allow accurate prediction of the premorbid morphology of the glenoid. This could help optimize implant selection and positioning after aTSA and rTSA to restore optimal soft-tissue tension.

Disclaimers:

Funding: No funding was disclosed by the authors.

Conflicts of interest: Jean-David Werthel and Gilles Walch are paid consultants and receive royalties for shoulder arthroplasty design from Stryker. Theo Giraudon, Manuel Urvoy, and Yannick Morvan are paid employees of Stryker. The other authors, their immediate families, and any research foundation with which they are affiliated have not received any financial payments or other benefits from any commercial entity related to the subject of this article.

REFERENCES

1. Abler D, Berger S, Terrier A, Becce F, Farron A, Buchler P. A statistical shape model to predict the premorbid glenoid cavity. J Shoulder Elbow Surg 2018;27:1800–8. https://doi.org/10.1016/j.jse.2018.04.023.
2. Bercik MJ, Kruse K 2nd, Yalizis M, Gauci MO, Chaoui J, Walch G. A modification to the Walch classification of the glenoid in primary glenohumeral osteoarthritis using three-dimensional imaging. J Shoulder Elbow Surg 2016;25:1601–6. https://doi.org/10.1016/j.jse.2016.03.010.
3. Berhouet J, Jacquot A, Walch G, Deransart P, Favard L, Gauci MO. Preoperative planning of baseplate position in reverse shoulder arthroplasty: still no consensus on lateralization, version and inclination. Orthop Traumatol Surg Res 2022;108:103115. https://doi.org/10.1016/j.otsr.2021.103115.
4. Boileau P, Cheval D, Gauci MO, Holzer N, Chaoui J, Walch G. Automated three-dimensional measurement of glenoid version and inclination in arthritic shoulders. J Bone Joint Surg Am 2018;100:57–65. https://doi.org/10.2106/JBJS.16.01122.
5. Boileau P, Gauci MO, Wagner ER, Clowez G, Chaoui J, Chelli M, et al. The reverse shoulder arthroplasty angle: a new measurement of glenoid inclination for reverse shoulder arthroplasty. J Shoulder Elbow Surg 2019;28:1281–90. https://doi.org/10.1016/j.jse.2018.11.074.
6. Clavert P, Millett PJ, Warner JJ. Glenoid resurfacing: what are the limits to asymmetric reaming for posterior erosion? J Shoulder Elbow Surg 2007;16:843–8. https://doi.org/10.1016/j.jse.2007.03.015.
7. Codsi MJ, Bennetts C, Gordiev K, Boeck DM, Kwon Y, Brems J, et al. Normal glenoid vault anatomy and validation of a novel glenoid implant shape. J Shoulder Elbow Surg 2008;17:471–8. https://doi.org/10.1016/j.jse.2007.08.010.
8. Cootes TF, Taylor CJ, Cooper DH, Graham J. Active shape models-their training and application. Comput Vis Image Understand 1995;61:38–59.
9. Edwards TB, Trappey GJ, Riley C, O'Connor DP, Elkousy HA, Gartsman GM. Inferior tilt of the glenoid component does not decrease scapular notching in reverse shoulder arthroplasty: results of a prospective randomized study. J Shoulder Elbow Surg 2012;21:641–6. https://doi.org/10.1016/j.jse.2011.08.057.
10. Elmallah R, Swanson D, Le K, Kirsch J, Jawa A. Baseplate retroversion does not affect postoperative outcomes after reverse shoulder arthroplasty. J Shoulder Elbow Surg 2022;31:2082–8. https://doi.org/10.1016/j.jse.2022.02.043.
11. Erickson BJ, Chalmers PN, Denard P, Lederman E, Horneff G, Werner BC, et al. Does commercially available shoulder arthroplasty preoperative planning software agree with surgeon measurements of version, inclination, and subluxation? J Shoulder Elbow Surg 2021;30:413–20. https://doi.org/10.1016/j.jse.2020.05.027.
12. Erickson BJ, Werner BC, Griffin JW, Gobezie R, Lederman E, Sears BW, et al. A comprehensive evaluation of the association of radiographic measures of lateralization on clinical outcomes following reverse total shoulder arthroplasty. J Shoulder Elbow Surg 2022;31:963–70. https://doi.org/10.1016/j.jse.2021.10.010.
13. Farron A, Terrier A, Buchler P. Risks of loosening of a prosthetic glenoid implanted in retroversion. J Shoulder Elbow Surg 2006;15:521–6. https://doi.org/10.1016/j.jse.2005.10.003.
14. Friedman RJ, Sun S, She X, Esposito J, Eichinger J, Yao H. Effects of increased retroversion angle on glenoid baseplate fixation in reverse total shoulder arthroplasty: a finite element analysis. Semin Arthroplasty 2021;31:209–16. https://doi.org/10.1053/j.sart.2020.11.014.
15. Giles JW, Langohr GD, Johnson JA, Athwal GS. The rotator cuff muscles are antagonists after reverse total shoulder arthroplasty. J Shoulder Elbow Surg 2016;25:1592–600. https://doi.org/10.1016/j.jse.2016.02.028.
16. Giles JW, Langohr GD, Johnson JA, Athwal GS. Implant design variations in reverse total shoulder arthroplasty influence the required deltoid force and resultant joint load. Clin Orthop

Relat Res 2015;473:3615–26. https://doi.org/10.1007/s11999-015-4526-0.
17. Giraudon T, Morvan Y, Walch A, Walch G, Werthel JD. Premorbid glenoid anatomy reconstruction from contralateral shoulder 3-dimensional measurements: a computed tomography scan analysis of 260 shoulders. J Shoulder Elbow Surg 2024;33:792–7. https://doi.org/10.1016/j.jse.2023.09.010.
18. Greiner S, Schmidt C, Herrmann S, Pauly S, Perka C. Clinical performance of lateralized versus non-lateralized reverse shoulder arthroplasty: a prospective randomized study. J Shoulder Elbow Surg 2015;24:1397–404. https://doi.org/10.1016/j.jse.2015.05.041.
19. Greiner S, Schmidt C, Konig C, Perka C, Herrmann S. Lateralized reverse shoulder arthroplasty maintains rotational function of the remaining rotator cuff. Clin Orthop Relat Res 2013;471:940–6. https://doi.org/10.1007/s11999-012-2692-x.
20. Gutierrez S, Comiskey CA, Luo ZP, Pupello DR, Frankle MA. Range of impingement-free abduction and adduction deficit after reverse shoulder arthroplasty. Hierarchy of surgical and implant-design-related factors. J Bone Joint Surg Am 2008;90:2606–15. https://doi.org/10.2106/JBJS.H.00012.
21. Gutierrez S, Walker M, Willis M, Pupello DR, Frankle MA. Effects of tilt and glenosphere eccentricity on baseplate/bone interface forces in a computational model, validated by a mechanical model, of reverse shoulder arthroplasty. J Shoulder Elbow Surg 2011;20:732–9. https://doi.org/10.1016/j.jse.2010.10.035.
22. Helmkamp JK, Bullock GS, Amilo NR, Guerrero EM, Ledbetter LS, Sell TC, et al. The clinical and radiographic impact of center of rotation lateralization in reverse shoulder arthroplasty: a systematic review. J Shoulder Elbow Surg 2018;27:2099–107. https://doi.org/10.1016/j.jse.2018.07.007.
23. Hettrich CM, Permeswaran VN, Goetz JE, Anderson DD. Mechanical tradeoffs associated with glenosphere lateralization in reverse shoulder arthroplasty. J Shoulder Elbow Surg 2015;24:1774–81. https://doi.org/10.1016/j.jse.2015.06.011.
24. Hill JM, Norris TR. Long-term results of total shoulder arthroplasty following bone-grafting of the glenoid. J Bone Joint Surg Am 2001;83:877–83.
25. Ho JC, Ricchetti ET, Iannotti JP. Central-peg radiolucency progression of an all-polyethylene glenoid with hybrid fixation in anatomic total shoulder arthroplasty is associated with clinical failure and reoperation. J Shoulder Elbow Surg 2021;30:1068–77. https://doi.org/10.1016/j.jse.2020.07.039.
26. Hoenecke HR Jr., Flores-Hernandez C, D'Lima DD. Reverse total shoulder arthroplasty component center of rotation affects muscle function. J Shoulder Elbow Surg 2014;23:1128–35. https://doi.org/10.1016/j.jse.2013.11.025.
27. Iannotti J, Baker J, Rodriguez E, Brems J, Ricchetti E, Mesiha M, et al. Three-dimensional preoperative planning software and a novel information transfer technology improve glenoid component positioning. J Bone Joint Surg Am 2014;96:e71. https://doi.org/10.2106/JBJS.L.01346.
28. Iannotti JP, Greeson C, Downing D, Sabesan V, Bryan JA. Effect of glenoid deformity on glenoid component placement in primary shoulder arthroplasty. J Shoulder Elbow Surg 2012;21:48–55. https://doi.org/10.1016/j.jse.2011.02.011.
29. Iannotti JP, Jun BJ, Derwin KA, Ricchetti ET. Stepped augmented glenoid component in anatomic total shoulder arthroplasty for B2 and B3 glenoid pathology: a study of early outcomes. J Bone Joint Surg Am 2021;103:1798–806. https://doi.org/10.2106/JBJS.20.01420.
30. Iannotti JP, Spencer EE, Winter U, Deffenbaugh D, Williams G. Prosthetic positioning in total shoulder arthroplasty. J Shoulder Elbow Surg 2005;14(1 Suppl S):111S–21S. https://doi.org/10.1016/j.jse.2004.09.026.
31. Iannotti JP, Weiner S, Rodriguez E, Subhas N, Patterson TE, Jun BJ, et al. Three-dimensional imaging and templating improve glenoid implant positioning. J Bone Joint Surg Am 2015;97:651–8. https://doi.org/10.2106/JBJS.N.00493.
32. Keener JD, Patterson BM, Orvets N, Aleem AW, Chamberlain AM. Optimizing reverse shoulder arthroplasty component position in the setting of advanced arthritis with posterior glenoid erosion: a computer-enhanced range of motion analysis. J Shoulder Elbow Surg 2018;27:339–49. https://doi.org/10.1016/j.jse.2017.09.011.
33. Luedke C, Kissenberth MJ, Tolan SJ, Hawkins RJ, Tokish JM. Outcomes of anatomic total shoulder arthroplasty with B2 glenoids: a systematic review. JBJS Rev 2018;6:e7. https://doi.org/10.2106/JBJS.RVW.17.00112.
34. Nunes B, Linhares D, Costa F, Neves N, Claro R, Silva MR. Lateralized versus nonlateralized glenospheres in reverse shoulder arthroplasty: a systematic review with meta-analysis. J Shoulder Elbow Surg 2021;30:1700–13. https://doi.org/10.1016/j.jse.2020.09.041.
35. Nyffeler RW, Sheikh R, Atkinson TS, Jacob HA, Favre P, Gerber C. Effects of glenoid component version on humeral head displacement and joint reaction forces: an experimental study. J Shoulder Elbow Surg 2006;15:625–9. https://doi.org/10.1016/j.jse.2005.09.016.
36. Parsons M, Greene A, Polakovic S, Rohrs E, Byram I, Cheung E, et al. Intersurgeon and intrasurgeon variability in preoperative planning of anatomic total shoulder arthroplasty: a quantitative comparison of 49 cases planned by 9 surgeons. J Shoulder Elbow Surg 2020;29:2610–8. https://doi.org/10.1016/j.jse.2020.04.010.
37. Plessers K, Vanden Berghe P, Van Dijck C, Wirix-Speetjens R, Debeer P, Jonkers I, et al. Virtual reconstruction of glenoid bone defects using a statistical shape model. J Shoulder Elbow Surg 2018;27:160–6. https://doi.org/10.1016/j.jse.2017.07.026.
38. Salhi A, Burdin V, Boutillon A, Brochard S, Mutsvangwa T, Borotikar B. Statistical shape modeling approach to predict missing scapular bone. Ann Biomed Eng 2020;48:367–79. https://doi.org/10.1007/s10439-019-02354-6.
39. Scalise JJ, Bryan J, Polster J, Brems JJ, Iannotti JP. Quantitative analysis of glenoid bone loss in osteoarthritis using three-dimensional computed tomography scans. J Shoulder Elbow Surg 2008;17:328–35. https://doi.org/10.1016/j.jse.2007.07.013.
40. Scalise JJ, Codsi MJ, Bryan J, Brems JJ, Iannotti JP. The influence of three-dimensional computed tomography images of the shoulder in preoperative planning for total shoulder arthroplasty. J Bone Joint Surg Am 2008;90:2438–45. https://doi.org/10.2106/JBJS.G.01341.
41. Sirveaux F, Favard L, Oudet D, Huquet D, Walch G, Mole D. Grammont inverted total shoulder arthroplasty in the treatment of glenohumeral osteoarthritis with massive rupture of the cuff. Results of a multicentre study of 80 shoulders. J Bone Joint Surg Br 2004;86:388–95. https://doi.org/10.1302/0301-620x.86b3.14024.
42. Szabo I, Buscayret F, Edwards TB, Nemoz C, Boileau P, Walch G. Radiographic comparison of flat-back and convex-back glenoid components in total shoulder arthroplasty. J Shoulder Elbow Surg 2005;14:636–42. https://doi.org/10.1016/j.jse.2005.05.004.
43. Terrier A, Ramondetti S, Merlini F, Pioletti DD, Farron A. Biomechanical consequences of humeral component malpositioning after anatomical total shoulder arthroplasty. J Shoulder Elbow Surg 2010;19:1184–90. https://doi.org/10.1016/j.jse.2010.06.006.
44. Verhaegen F, Plessers K, Verborgt O, Scheys L, Debeer P. Can the contralateral scapula be used as a reliable template to reconstruct the eroded scapula during shoulder arthroplasty? J Shoulder Elbow Surg 2018;27:1133–8. https://doi.org/10.1016/j.jse.2017.12.024.

45. Walch G, Badet R, Boulahia A, Khoury A. Morphologic study of the glenoid in primary glenohumeral osteoarthritis. J Arthroplasty 1999;14:756–60.
46. Walch G, Moraga C, Young A, Castellanos-Rosas J. Results of anatomic nonconstrained prosthesis in primary osteoarthritis with biconcave glenoid. J Shoulder Elbow Surg 2012;21:1526–33. https://doi.org/10.1016/j.jse.2011.11.030.
47. Werthel JD, Walch G, Vegehan E, Deransart P, Sanchez-Sotelo J, Valenti P. Lateralization in reverse shoulder arthroplasty: a descriptive analysis of different implants in current practice. Int Orthop 2019;43:2349–60. https://doi.org/10.1007/s00264-019-04365-3.
48. Williams GR Jr., Wong KL, Pepe MD, Tan V, Silverberg D, Ramsey ML, et al. The effect of articular malposition after total shoulder arthroplasty on glenohumeral translations, range of motion, and subacromial impingement. J Shoulder Elbow Surg 2001;10:399–409.
49. Yongpravat C, Kim HM, Gardner TR, Bigliani LU, Levine WN, Ahmad CS. Glenoid implant orientation and cement failure in total shoulder arthroplasty: a finite element analysis. J Shoulder Elbow Surg 2013;22:940–7. https://doi.org/10.1016/j.jse.2012.09.007.